EFDA–JET–PR(07)53

D. Kalupin, S. Wiesen, Y. Andrew, M.Z. Tokar, V. Parail, D. Reiser, G. Corrigan,
A. Korotkov, J. Spence and JET EFDA contributors

Edge Transport Barrier Formation Studies on JET with the JETTO Code

Edge Transport Barrier Formation Studies on JET with the JETTO Code

D. Kalupin[1], S. Wiesen[1], Y. Andrew[2], M.Z. Tokar[1], V. Parail[2], D. Reiser[1], G. Corrigan[2], A. Korotkov[2], J. Spence[2] and JET EFDA contributors*

JET-EFDA, Culham Science Centre, OX14 3DB, Abingdon, UK

[1]Institut für Energieforschung – 4 (Plasmaphysik), Forschungszentrum J¸lich GmbH, EURATOM Association, D-52425 Jülich, Germany, partner in Trilateral Euregio Cluster
[2]EURATOM-UKAEA Fusion Association, Culham Science Centre, OX14 3DB, Abingdon, OXON, UK
** See annex of M.L. Watkins et al, "Overview of JET Results ",*
(Proc. 21 st IAEA Fusion Energy Conference, Chengdu, China (2006)).

Preprint of Paper to be submitted for publication in
Nuclear Fusion

ABSTRACT.
The 1.5D transport code JETTO [1] has been applied to model the transition from the low (L) to the high confinement mode (H-mode) in the JET tokamak. Computed values of the critical power, P_{th}, required for the L-H transition on JET are directly compared with experiment [2] across line averaged density and magnetic field scans. Reasonable agreement is found between computations and experiment across all densities considered, including low density discharges, where P_{th} increases with decreasing density. The minimum of P_{th} (n_e) dependence is explained by the enhanced contribution of the particle convection to heat losses at the edge. Higher convective losses result in lower temperature and its gradient, and therefore more power is required for the L-H transition. Computations performed for JET discharges with varied magnetic field show a rough agreement with the experiment, nonetheless both computed and experimental power threshold are substantially higher than the inter-machine scaling predictions [3].

1. INTRODUCTION

The H-mode [4] is a regime characterized by substantially improved plasma confinement, which is caused by a strong reduction in anomalous transport at the plasma periphery. This regime is generally obtained if the total heating power exceeds some characteristic level, determined by the plasma density, magnetic field and plasma outer area [3]. A large number of transport models that try to explain the self-organised improvement of confinement in the H-mode have been constructed since the regime was discovered. Models developed before the year 2000 have been reviewed by Connor et al in [5]. Later, a few of them were tested against experimental data obtained on the MAST tokamak [6]. In spite of different mechanisms leading to the turbulence suppression, all analyzed models predicted substantial reduction of transport after L to H-mode transition. Nevertheless, this does not prove the capability of the model to predict the L-H transition. Indeed, in all considered models the critical parameters that determine the conditions for transport suppression are controlled by edge plasma parameter gradients. These gradients are always strongly altered following the L-H transition and thus all models naturally separate the L and H-mode data.

In order to demonstrate the capability of a transport model to predict the L-H transition, it should be introduced into a transport code, and the result of predictive computations should be compared with experiment. This approach was used in [7-10], where the transport model that allows for the formation of the Edge Transport Barrier (ETB) was introduced to the 1.5-D transport code RITM [7,11]. The computations performed for the conditions of the limiter tokamak TEXTOR were capable of predicting the power threshold for the L-H transition, confirmed later in experiment [7].

This approach has been extended to JET by coupling the RITM model to the 1.5D transport code JETTO. This paper presents first results on the modeling of the ETB formation in the JET tokamak with the coupled JETTO-RITM transport code. Computations have been performed to compare the results from the modeling with experiment on JET. Discharges with various magnetic field and plasma density have been analyzed. Results are also compared to the inter-machine scaling law [3], which

summarizes data from several tokamaks.

The remainder of this paper is organized as follows. Section II introduces the numerical tools used in our studies. Section III compares the computed L-H power threshold with the experimental one and with values predicted by the inter-machine scaling. Section IV discusses the minimum of the L-H power threshold observed in JET discharges at low density. Conclusions are given in Section V.

2. NUMERICAL TOOLS USED IN COMPUTATIONS

The 1.5-D transport code JETTO [1] allows for the modeling of the time evolution of different plasma parameter profiles. It solves transport equations averaged over magnetic surfaces for electron and ion temperatures, ion density and ion toroidal velocity. The magnetic configuration is determined by the Grad-Shafranov equation, using computed density and temperature profiles. The charged particle sources are described by the integral equation for the energy distribution function of neutrals solved by the FRANTIC code [12]. The power deposition profiles are taken from experiment. In order to perform the power scan, they are scaled by numerical factors. The boundary conditions, e.g. densities and temperatures at the Last Closed Magnetic Surface (LCMS) and the neutral influx from the Scrape-Off Layer (SOL) in the confined plasma, are calculated with the two-dimensional transport code EDGE2D, which solves fluid equations for the SOL plasmas, coupled with the 2-D Monte Carlo solver NIMBUS describing the particle and energy sources in the SOL due to recycling and puffed neutrals [13].

Transport coefficients for equations solved by the JETTO code are computed with the package extracted from the RITM code [7,8]. Its model accounts for drift instabilities of different nature, e.g. Ion Temperature Gradient (ITG) and Trapped Electron (TE) modes, which are considered to be responsible for the transport in the plasma core, and for the modes driven by collisions and current perturbations, like Drift Resistive Ballooning (DRB) and Drift Alfven (DA) instabilities, which are dominating the anomalous transport at the plasma edge under the L-mode conditions. For each unstable drift mode a dispersion equation for the complex frequency as a function of the wave vector perpendicular to the magnetic field, k, is analytically derived from transport equations linearized to small perturbations of plasma parameters. Dispersion equations for all unstable modes are solved numerically. For every mode the perturbation with the maximum growth rate $\gamma^{ITG,\,TE,\,Edge} = \max\,(\gamma(k))_{ITG,\,TE,\,Edge}$ is selected. The individual transport coefficients caused by different instabilities are estimated using the mixing length approximation [14],

$$\chi_{\perp}^{ITG,\,TE,\,Edge} = \frac{\gamma^{\,ITG,\,TE,\,Edge}}{k^{2}_{ITG,\,TE,\,Edge}} \cdot R_{E\times B}^{ITG,\,TE,\,Edge}, \qquad (1)$$

from the maximum growth rate and the perpendicular wave number at which the maximum values are achieved, $k^{ITG,\,TE,\,Edge}$. $R_{E\times B}^{ITG,\,TE,\,Edge} = C^{ITG,\,TE,\,Edge} \cdot (1+(\omega_{E\times B}/\varepsilon\gamma_{ITG,\,TE,\,Edge})^{2})^{-1}$ are the normalisation factors for particular instabilities, accounting for the suppression of the turbulent transport by the

shear of the radial electric field, $\omega_{E\times B} = \frac{RB_\vartheta}{B}\frac{\partial}{\partial r}\left(\frac{E_r}{RB_\vartheta}\right)$ [15]. Here, $C^{ITG,\,TE,\,Edge}$ are the weights of individual instability in the total transport coefficient, chosen by fitting of computed profiles of the density and temperature to the measurements, and ε is a factor between 0.5 and 2, R and r are the major and minor plasma radii respectively. The radial electric field is computed from the force balance equation:

$$E_r = \frac{V_\varphi V_\vartheta - V_\vartheta V_\varphi}{c} + \frac{1}{en_i}\frac{\partial (n_i T_i)}{\partial r} \tag{2}$$

where e is the elementary charge, c is a speed of light, n_i, T_i are the ion density and temperature and $B_{\vartheta,\varphi}$ are the poloidal and toroidal components of the magnetic field. The neoclassical poloidal rotation, V_ϑ, is calculated by the NCLASS package [16] coupled with the JETTO code, following the formulation given in [17]. The toroidal rotation, V_φ, is set to zero in present computations.
The total transport coefficients are taken in the form:

$$\kappa_\perp^i = \kappa_\perp^{iNEO} + (\chi^{ITG} + \chi^{TE} + \chi^{edge} + C^{core})n_i, \tag{3}$$

$$\kappa_\perp^i = \kappa_\perp^{iNEO} + (\chi^{ITG} + \chi^{TE} + \chi^{edge} + C^{core})n_i, \tag{4}$$

$$D_\perp^i = D_\perp^{iNEO} + 2/3\,(\chi^{ITG} f_{tr} + \chi^{TE} + \chi^{edge} + C^{core}). \tag{5}$$

Here, $\kappa^{e,i}$ are the electron and ion heat conductivities, $D^I_\perp$ is the ion diffusion coefficient. The neoclassical heat conductivity, $\kappa_\perp^{i,\,NEO}$, and particle diffusion coefficient, $D_\perp^{i,\,NEO}$, are computed by the NCLASS code. Since the neoclassical transport for electrons is very low, its contribution is considered in the ion transport channel only. Nevertheless, within the transport barrier the electron transport is assumed of the order of ion neoclassical transport. The ad hoc background transport of a very low level, $C^{core} = 0.1\text{m}^2/\text{s}$, is added within $q = 1$ magnetic surface in order to avoid a zero transport coefficients on axis, which might result from flat central profiles, that would provide numerical difficulties for computations.

Present transport model predicts strong reduction of the turbulent transport at the edge and the transition to the H-mode if the total heating power is above some critical level. At low heating power, high collisionality provides a strong drive for DA and DRB modes dominating the turbulent transport at the plasma edge. The increase of the heating leads to increase of temperature and of its gradient and decrease of collisionality. This reduces the turbulent transport at the edge driven by DA and DRB instabilities. Lower transport leads to further increase of the temperature and its gradient, and, finally, causes the quench of the turbulent transport at the edge. Increased gradient of pressure at the edge leads to the increase of the radial electric field, eq.(2). This provides the mechanism for the turbulence suppression [15], additional to the one by the temperature gradient. It is very difficult to point out the

unique mechanism which dominates the ETB formation, as both of them are very strongly coupled. Nevertheless, it was shown in [7] that, the present transport model allows for the ETB formation even with $\omega_{E\times B} = 0$, whereas the $E\times B$ term alone does not allow for the formation of a pronounced barrier. Moreover, local analysis, in which the stabilization by the $E\times B$ shear was omitted, predicts variation of the critical power, at which the turbulent transport is suppressed, in agreement with the inter-machine scaling for the L-H transition [8].

In order to adjust free normalization factors $C^{ITG,TE,Edge}$ weighting contributions from individual modes to total transport coefficients, the L-mode phase (time = 20.2s) of JET Pulse No: 58764 was simulated. The power deposition profiles and the particle source from the neutral beam injection have been taken from the experiment. The total heating power was 5.1MW, the toroidal magnetic field 2.68T and the total plasma current 2.56MA. Plasma parameters at the LCMS have been computed by the EDGE2D-NIMBUS package, taking the experimental heat flux from the core to the scrape-off layer, magnetic geometry and the gas puffing rate into account.

Figure 1 shows profiles of ion and electron temperatures and contributions to the ion heat transport coefficient, anomalous, provided by the RITM model, and neoclassical, provided by the NCLASS. It is seen that, both temperatures, for electrons and ions, are reproduced in close agreement with experimental profiles. The following model settings have been chosen in the computations presented in fig.1. Normalization constants for the ITG and TE modes are $C^{ITG,\,TE} = 2.88$ and for the edge instabilities, $C^{Edge} = 30$. The proportionality coefficient e determining the ratio between instability growth rate and the E×B shearing rate, at which the stabilization of the turbulent transport occurs, is set to 0.5. These settings adjusted for the singular shot were kept fixed through all computations presented in the paper.

3. COMPARISON OF COMPUTED POWER THRESHOLD TO THE JET EXPERIMENTAL RESULTS

The modeling of the L to H-mode transition with the JETTO code has been performed for two series of JET discharges. In the first series the edge density has been varied at fixed magnetic field and plasma current and in the second one the variation of the magnetic field at fixed edge safety factor has been done. For all shots chosen for the analysis, a power scan with the step of 0.5MW has been performed in order to determine the power threshold for the L-H transition. This was done by scaling the heat deposition profiles obtained from the experiment. Figure 2 presents an example of such a power scan done for the conditions of the discharge shown in fig.1. It shows the ion heat diffusion coefficient at the edge, ion temperature and electron density at the pedestal top, gradients of temperature and density in the barrier region and the ballooning parameter, α/α_{ball}, versus the total heating power.

Here $\alpha = \frac{8\pi R q^2}{B_T^2}\left|\frac{\partial(n_e T_e + n_i T_i)}{dr}\right|$ is the normalized pressure gradient and $\alpha_{ball} = 0.4 s_{95}\,[1 + \delta_{95}{}^2(1+5\kappa_{95}{}^2)]$ is the ideal ballooning limit, q is the safety factor, and s_{95}, and κ_{95} are the values of the magnetic shear, elongation and triangularity at the magnetic surface where the toroidal flux is

95% of its value at the LCMS. According to Ref. [18], $\delta_{95} = 0.914\delta_{separatrix}$ and $\kappa_{95} = 0.85\kappa_{separatrix}$, with $\delta_{separatrix}$ and $\delta_{separatrix}$ being the values at the LCMS.

While the total heating power increases, the ion heat transport coefficient at the edge remains practically unchanged at the level of 1.5-1.8 m^2s^{-1}, up to the heating power of 6.5MW. Strong turbulent transport results in the low temperature and low pressure gradient at the edge, the latter stays far below the ideal ballooning limit. The increase of the power up to 6.9MW leads to the sudden drop of the turbulent transport coefficient, and to the substantial increase of the temperature and its gradient at the edge. The edge density increases slightly, but the change is much weaker than it is seen in the temperature. Reduction of the turbulent transport results mainly in more steep edge density profile. For the heating power above 6.9MW, the gradient of the total pressure overcomes the ideal ballooning limit, which is considered to be the criteria for the onset of Edge Localized Mode (ELM) of the type I. Because computations were aimed at determining the critical heating power for the L-H transition only, and not in the modeling of plasma profiles in H-mode, where the ELM activity is playing a crucial role in determining plasma parameters at the edge, ELM modeling was ignored in present studies. Therefore, the normalized pressure gradient in fig.2 grows above the ideal ballooning limit.

For further analysis of the variation of the L-H threshold power with plasma parameters, the definition for L-H transition should be given. Often, the appearance of the regular ELM activity, which remains longer than the single sawtooth period, is selected as experimental criteria for the L-H transition [2,19]. In present studies we adopt this criteria assuming that ELMs should appear for $\alpha/\alpha_{ball} \geq 1$. Thus the L-H threshold can bedefined as the minimum heating power at which the normalized pressure gradient overcomes the ballooning limit,$P_{th} = \min [P_{heat}(\alpha/\alpha_{ball} \geq 1)]$.

Transport modeling requires the knowledge of plasma parameters at the Last Closed Flux Surface (LCFS) which are used as the boundary conditions for computations. Moreover, the L to H-mode transition is an edge phenomenon and can be extremely sensitive to the choice of boundary quantities [8,9]. Profiles of edge parameters measured in experiment are, usually, very noisy, that can impose a large uncertainty on modeling results. Also, some of the required quantities are not measured. Thus, discharges selected for the transport modeling were first analyzed with the 2-D transport code package EDGE2d/NIMBUS in order to calibrate edge profiles on physics-based model. The magnetic geometry, neutral puff and energy flux in to the SOL have been taken from the experiment. The heat and particle transport coefficients have been provided by JETTO computations and assumed constant over the SOL region. Figure 3 shows the plasma parameters averaged over the last closed magnetic surface, obtained with EDGE2d/NIMBUS package for the sequence of JET discharges with different edge density, measured a few centimeters inside the LCFS. Most of computed quantities are weakly dependent on the edge density, except for the density at the LCMS, which increases linearly and being about 70% of the edge density. The neutral influx into confined plasma is only a few percents of the flux released by walls and similar for all of considered discharges. Figure 4 shows the same set of edge parameters computed for discharges with different values of toroidal magnetic field. The edge density was not controlled in these discharges, thus, computed density at the LCFS has some variation

over the sequence. The higher heat flux in to the SOL and lower density lead to higher temperatures for discharges at high magnetic field. The computed neutral flux through the LCFS varies by ~25% between different shots.

Results of predictive transport modeling with the JETTO code, using boundary values shown in fig. 3 and 4, are presented in fig.5 and 6. Figure 5 compares power threshold at different value of the edge density obtained in computations to the one from experiment and the one predicted by the inter-machine scaling. The latter was obtained from the expression: $P_{th}[MW] = 0.042\bar{n}_e^{0.64}B^{0.78}S^{0.94}$, where $\bar{n}_e$ is the line averaged electron density in $10^{20}\mathrm{m}^{-3}$, S the plasma surface area in m^2, and B the toroidal magnetic field in T [3]. For the whole range of densities, values obtained with the transport model, adjusted for one particular discharge, are in agreement with experimental and scaling values. All three sequences of points coincide within error bars; except for the highest density case, where the value predicted by the scaling law is about 30% lower than experimental and computed values. This difference is most probably due to the divertor configuration [21] different to the one in earlier JET discharges used in the data base for scaling construction. The change of the divertor configuration, particularly of the X-point location, results in strong modification of particle fluxes through the LCFS, and thus, can prohibit the L-H transition [8].

Computations done for the sequence of discharges with different magnetic field are shown in fig.6. It is important to note that, keeping the model setting fixed, the switch to plasma conditions, substantially different from the one in fig.5, did not break the agreement between experimental and numerical results. The experimental variation of the power threshold for the L-H transition is well reproduced by the modelling. Nonetheless, there is a substantial difference to the value of the critical power predicted by the inter-machine scaling under all conditions, although trends between different curves agree. Higher experimental values can be explained by the influence of divertor geometry not taken into account by the general scaling law. Transport computations, where the actual geometry was used, reproduce experimental values in close agreement.

4. MINIMUM OF $P_{TH}(N_E)$ DEPENDENCE

The JETTO code has been also applied to model the L-H transition at a low density, when the threshold power increases with decreasing density [2]. The minimum of $P_{th}(n_e)$ dependence is a general feature observed in most tokamaks operating in H-mode. In [3] it was suggested that the deep penetration of recycling neutrals to the core plasma can be the reason for the increase of the L-H threshold towards low density. The multi-machine scaling for the L-H threshold power, predicting $P_{th} \sim n_e^{0.64}$, was constructed on a set of data that excludes the low density discharges, and thus, is not applicable for low density plasmas. Our previous computations with the RITM code for conditions of the TEXTOR tokamak [8], have confirmed the crucial role of neutrals in L-H transition in limiter devices. It was shown that, the strong convective heat losses due to charge particle transport is the key factor for the increase on the L-H threshold power [8,9]. Present studies show that the same mechanism leads to the increase of the L-H threshold in divertor tokamaks at low density.

Figure 7 presents the threshold power for the L-H transition and the fraction of convective losses in the total heat flux at the edge as a function of the density at the LCMS obtained in JETTO computations. The computed power decreases with decreasing density at the LCMS in agreement with the scaling prediction down to the densities about 0.7-0.8*$10^{19}$$m^{-3}$. This roughly correspond to experimentally measured densities at the pedestal top of ~ 1.1-1.3*$10^{19}$$m^{-3}$ [2]. At this density the $P_{th}(n_e)$ dependence has a minimum. Further decrease of density in computations resulted in the growth of the power threshold in agreement with JET experiment.

At low density the penetration of recycling neutrals to the core plasma increases due to weaker attenuation of the neutral flux released by walls in the divertor region and SOL. In steady state this leads to the increase of the charge particle losses, and thus, to the increase of convective loss of energy. The temperature gradient decreases, thus, higher heating power is required to reach the critical gradient of temperature at which the edge turbulence is suppressed. The fraction of convective energy losses, at which the minimum of $P_{th}(n_e)$ dependence is observed, is about 0.4. This roughly corresponds to the previously obtained 0.5 for TEXTOR conditions [8].

CONCLUSIONS

The RITM transport model that allows for the ETB formation has been introduced to the 1.5-D transport code JETTO. Predictive computations, done for series of JET discharges, show reasonable agreement with experiment across density and magnetic field scans. Calculations done for low density discharges support the conclusion made in [8] on the crucial role of neutrals in increase of L-H power threshold towards low density. The inter-machine scaling [3] for the L-H threshold power is applicable only for discharges where the heat losses are mostly due to heat conduction. Deep penetration of neutrals to confined plasma, at low density, enhances convective energy losses due to charged particle transport. This result in lower temperature and its gradient, and thus prohibit the L-H transition. The critical fraction of convective energy losses corresponding to the minimum of $P_{th}(n_e)$ dependence is about 0.4-0.5 of the total heat losses, for both TEXTOR [8] and JET.

REFERENCES

[1]. Cenacchi G., Taroni A., 1988, Rapporto ENEA RT/TIB (88)5

[2]. Andrew Y., *et al*, 2006, Plasma Phys. and Contr. Fusion **48** 479

[3]. ITPA H-mode Power Threshold Database Working Group presented by Takizuka T., 2004, Plasma Phys. and Contr. Fusion **46** A227

[4]. ASDEX team, 1989, Nucl. Fusion **29** 1959

[5]. Connor J.W. *et al*, 2000, Plasma Phys. and Contr. Fusion **42** R1

[6]. Meyer H., *et al*. 2006, Nuclear Fusion **46** 64

[7]. Kalupin D., Tokar *et al*, 2005, Nuclear Fusion **45** 468

[8]. Kalupin D., *et al*, 2006, Physics of Plasmas **13** 032504

[9]. Kalupin D., *et al*, 2006, Plasma Phys. and Contr. Fusion **48** A309

[10]. Kalupin D., *et al*, 2006, Contrib. Plasma Phys. **46** 685
[11]. Tokar M.Z., 1994, Plasma Phys. and Contr. Fusion **36** 1819
[12]. Tamor S., 1981, J. Computational Physics, **40** 104
[13]. Simonini R., *et al*, 1994, Contrib. Plasma Phys. **34** 368
[14]. Connor J.W. and PogutseO.P., 2001, Plasma Phys. and Contr. Fusion **43** 155
[15]. Terry P W, 2000, Rev. Mod. Phys. **72** 109
[16]. Houlberg W., *et al*. 1997, Physics of Plasmas **4** 3230
[17]. Hirshman S.P., *et al*. 1977, Nuclear Fusion **17** 611
[18]. Onjun T., *et al*, 2002, Phys. Plasmas **9** 5018
[19]. Andrew Y., *et al*, 2004, Plasma Phys. and Contr. Fusion **46** 337
[20]. Tokar M.Z., *et al*, 2005, Physics of Plasmas **12** 052510
[21]. Andrew Y.,*et al*, presentation at 12th Transport Physics Topical Group meeting, 7-10 May 2007, EPFL, Lausanne, Switzerland.

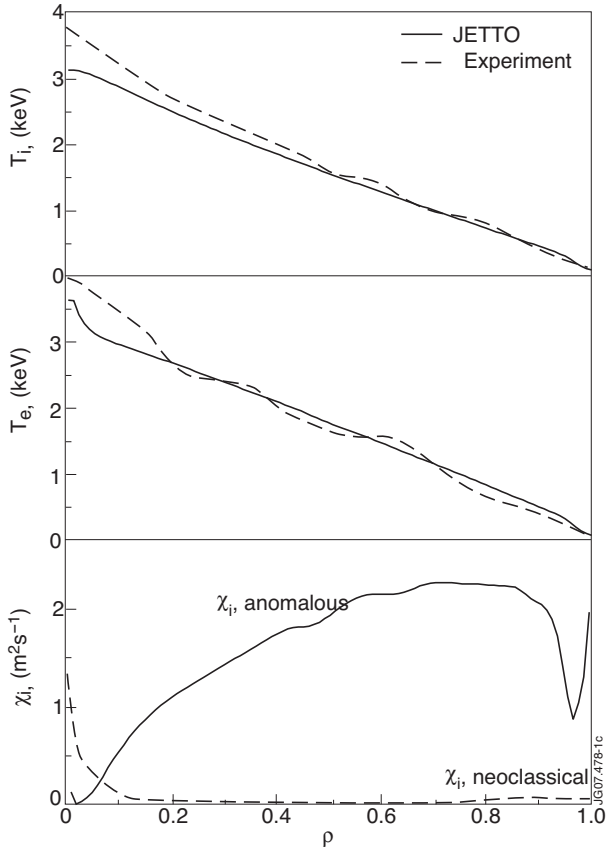

Figure 1: Experimental and computed profiles of the electron and ion temperatures and computed heat transport coefficients for L-mode JET plasma (Pulse No: 58764, time = 20.2 s., P_{heat}=5.1 MW)

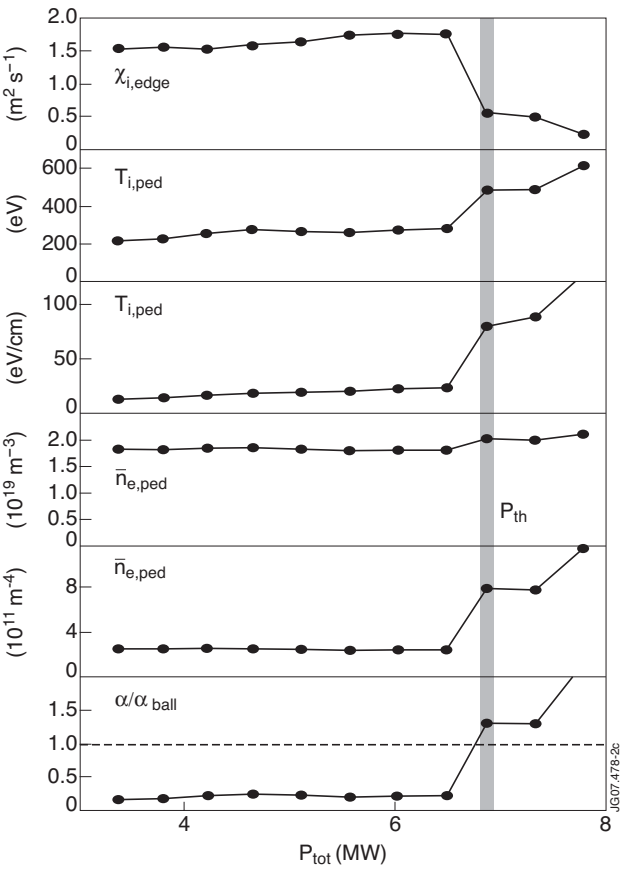

Figure 2: Power scan for conditions of JET Pulse No: 58764. Computed plasma parameters at the edge (ion heat diffusion coefficient, ion temperature and its gradient, electron density and its gradient and the maximum ballooning parameter) as a function of the total heating power. The threshold power is defined as the minimum power at which the normalized pressure gradient overcomes the ballooning limit, $\alpha/\alpha_{ball} \geq 1$.

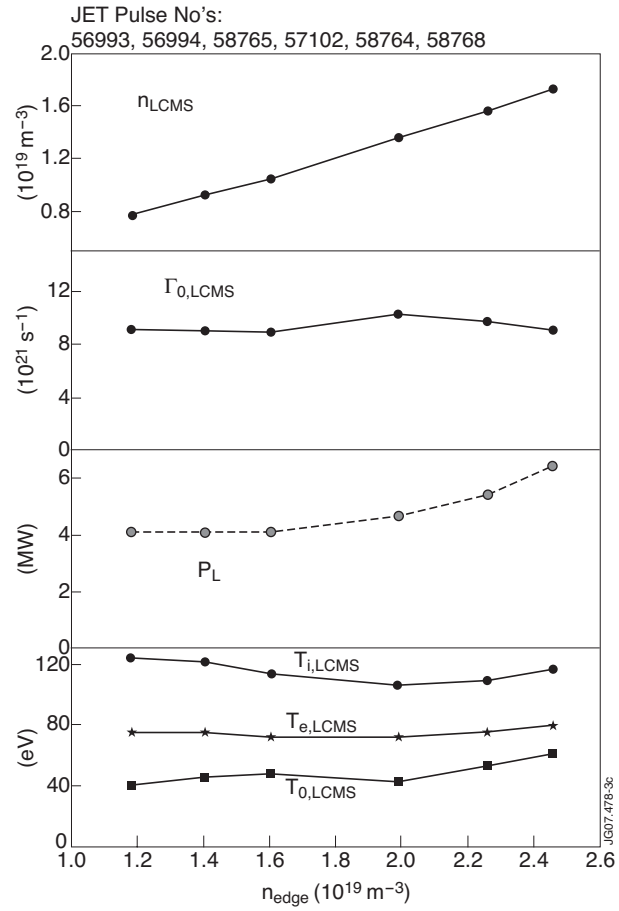

Figure 3: Plasma parameters at the LCFS computed with the EDGE2D-NIMBUS package, assuming experimental level of the gas puffing and heat flux from the core to the SOL region, for six JET discharges with different edge density.

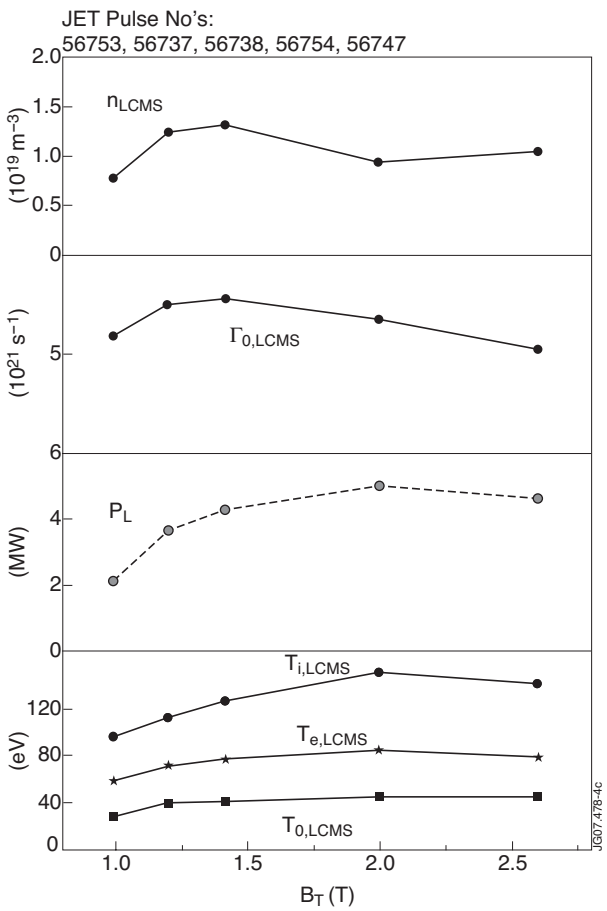

Figure 4: Plasma parameters at the LCFS computed with the EDGE2D-NIMBUS package, for JET discharges with various magnetic field.

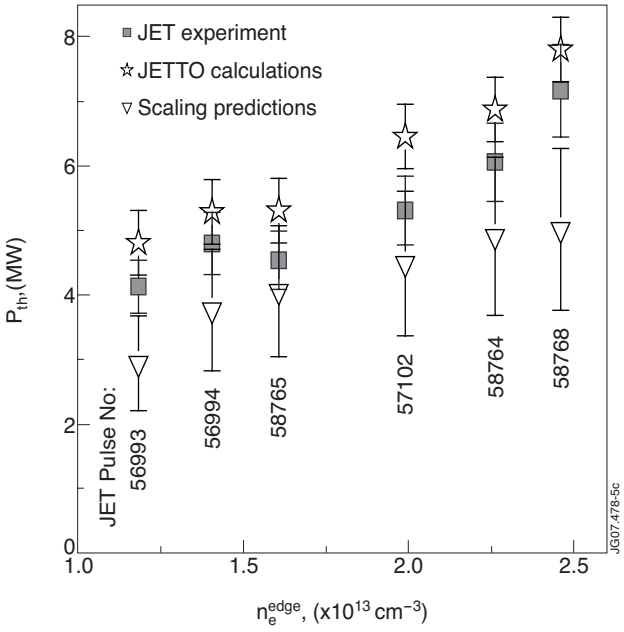

Figure 5: Comparison of the L-H power threshold computed with the JETTO code to the values obtained in experiment and predicted by the inter-machine scaling, for the set of discharges with various densities

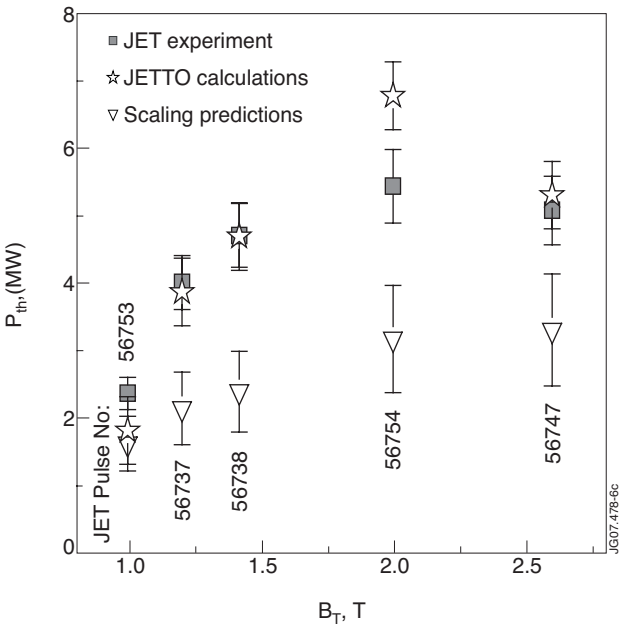

Figure 6: Comparison of the L-H power threshold computed with the JETTO code to the values obtained in experiment and predicted by the inter-machine scaling, for the set of discharges with various magnetic field.

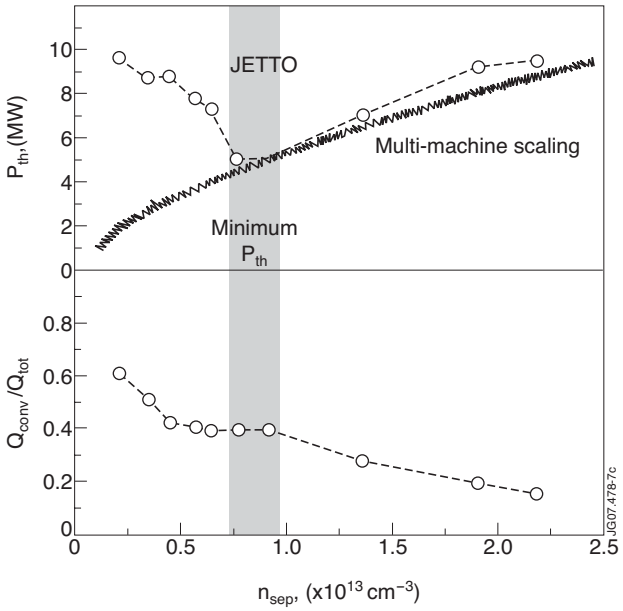

Figure 7: L-H power threshold obtained in JETTO computations using RITM model and predicted by multi-machine scaling, and the fraction of convective energy losses in the total one as a function of the density at the LCMS. The minimum of $P_{th}(n_e)$ dependence correspond to the critical fraction of convective heat losses at the edge, Q_{conv}/Q_{tot}~0.4.